

## Coassembly of Graphene Oxide and Nanowires for Large-Area Nanowire Alignment

Yanguang Li and Yiyang Wu\*

Department of Chemistry, The Ohio State University, 100 West 18th Avenue, Columbus, Ohio 43210

Received January 6, 2009; E-mail: wu@chemistry.ohio-state.edu

**Abstract:** We study the coassembly behavior of graphene oxide (GO) nanosheets and Na<sub>0.44</sub>MnO<sub>2</sub> nanowires. With the addition of GO nanosheets to the nanowire aqueous suspension, we observed the concentration enrichment and orientation alignment of nanowires at the air–water interface. The aligned nanowires can be transferred to hydrophilic substrates with their orientation parallel to the liquid–substrate contact line upon evaporation of the solvent. The underlying mechanism was studied carefully. GO nanosheets can be thought as “soft” two-dimensional macromolecules. Through hydrogen bonding and ion–dipole interactions, GO nanosheets can adsorb onto the nanowire surface and alter the surface properties. As a result, the GO-adsorbed nanowires become surface active and are enriched at the air–water interface. The adsorption of GO also increases the negative surface charge density of the nanowires and thus further stabilizes the colloidal solution. When a critical concentration is reached, the alignment of nanowires occurs according to Onsager’s theory. This study brings about a new application of GO in colloidal chemistry and a novel method to achieve large-area, unidirectional alignment of nanowires.

### Introduction

Recent advances in nanotechnology enable us to synthesize a variety of nanoparticles, nanorods, or nanowires with a narrow size/shape distribution and good colloidal stability<sup>1,2</sup> and, therefore, open up the possibility of systematically studying their assembly behaviors. For example, monodispersed quasi-spherical CdSe and CoPt<sub>3</sub> nanoparticles have been shown to self-organize into three-dimensional close-packed superlattices.<sup>3,4</sup> Anisotropic nanoparticles, such as nanorods, nanowires, and nanoplatelets, have the additional degree of freedom due to the orientation, which makes their phase behavior intrinsically richer than that of spherical nanoparticles. Onsager’s theory considers rods as noninteracting hard spherocylinders and predicts the formation of a series of orientationally and/or positionally ordered liquid crystal phases.<sup>5,6</sup> Self-alignment of nanorods of Ag,<sup>7</sup> Au,<sup>7–9</sup> Co,<sup>10</sup> CoO,<sup>11</sup> CdSe,<sup>12–14</sup> and CdS,<sup>14,15</sup> as well as

short carbon nanotubes,<sup>16</sup> has been experimentally observed in concentrated dispersion upon evaporation of solvent. With the increase of the aspect ratio, nanorods and nanowires become more difficult to self-assemble into structures with orientational and/or positional order due to the extra possible configurations such as curling and twisting associated with these long and flexible nanostructures. Therefore, external force is typically required to facilitate their assembly, such as Langmuir–Blodgett compression,<sup>17,18</sup> electric/magnetic field induction,<sup>19–21</sup> fluidic flow in microchannels,<sup>22</sup> and the stick–slip motion during solvent evaporation.<sup>23</sup> In addition to the assembly of spherical nanoparticles and nanorods, plate-like nanoparticles have also been observed to form liquid crystal phases in colloidal suspensions.<sup>24</sup>

The coassembly of mixed nano-objects with different sizes and/or shapes represents a fundamentally interesting topic: what

- (1) Yin, Y.; Alivisatos, A. P. *Nature (London)* **2005**, *437*, 664–670.
- (2) Xia, Y. N.; Yang, P. D.; Sun, Y. G.; Wu, Y. Y.; Mayers, B.; Gates, B.; Yin, Y. D.; Kim, F.; Yan, Y. Q. *Adv. Mater.* **2003**, *15*, 353–389.
- (3) Murray, C. B.; Kagan, C. R.; Bawendi, M. G. *Science* **1995**, *270*, 1335–1338.
- (4) Talapin, D. V.; Shevchenko, E. V.; Murray, C. B.; Titov, A. V.; Kral, P. *Nano Lett.* **2007**, *7*, 1213–1219.
- (5) Onsager, L. *Ann. N.Y. Acad. Sci.* **1949**, *51*, 627–659.
- (6) Frenkel, D. *J. Phys. Chem.* **1988**, *92*, 3280–3284.
- (7) Jana, N. R. *Angew. Chem., Int. Ed.* **2004**, *43*, 1536–1540.
- (8) Nikoobakht, B.; Wang, Z. L.; El-Sayed, M. A. *J. Phys. Chem. B* **2000**, *104*, 8635–8640.
- (9) Sau, T. K.; Murphy, C. J. *Langmuir* **2005**, *21*, 2923–2929.
- (10) Dumestre, F.; Chaudret, B.; Amiens, C.; Respaud, M.; Fejes, P.; Renaud, P.; Zurcher, P. *Angew. Chem., Int. Ed.* **2003**, *42*, 5213–5216.
- (11) An, K.; Lee, N.; Park, J.; Kim, S. C.; Hwang, Y.; Park, J. G.; Kim, J. Y.; Park, J. H.; Han, M. J.; Yu, J. J.; Hyeon, T. *J. Am. Chem. Soc.* **2006**, *128*, 9753–9760.
- (12) Li, L.-S.; Walda, J.; Manna, L.; Alivisatos, A. P. *Nano Lett.* **2002**, *2*, 557–560.

- (13) Talapin, D. V.; Shevchenko, E. V.; Murray, C. B.; Kornowski, A.; Forster, S.; Weller, H. *J. Am. Chem. Soc.* **2004**, *126*, 12984–12988.
- (14) Querner, C.; Fischbein, M. D.; Heiney, P. A.; Drndic, M. *Adv. Mater.* **2008**, *20*, 2308–2314.
- (15) Carbone, L. *Nano Lett.* **2007**, *7*, 2942–2950.
- (16) Shimoda, H.; Oh, S. J.; Geng, H. Z.; Walker, R. J.; Zhang, X. B.; McNeil, L. E.; Zhou, O. *Adv. Mater.* **2002**, *14*, 899–901.
- (17) Kim, F.; Kwan, S.; Akana, J.; Yang, P. *J. Am. Chem. Soc.* **2001**, *123*, 4360–4361.
- (18) Whang, D.; Jin, S.; Wu, Y.; Lieber, C. M. *Nano Lett.* **2003**, *3*, 1255–1259.
- (19) Acharya, S.; Patla, I.; Kost, J.; Efrima, S.; Golan, Y. *J. Am. Chem. Soc.* **2006**, *128*, 9294–9295.
- (20) Gupta, S.; Zhang, Q.; Emrick, T.; Russell, T. P. *Nano Lett.* **2006**, *6*, 2066–2069.
- (21) Smith, P. A.; Nordquist, C. D.; Jackson, T. N.; Mayer, T. S.; Martin, B. R.; Mbindyo, J.; Mallouk, T. E. *Appl. Phys. Lett.* **2000**, *77*, 1399–1401.
- (22) Huang, Y.; Duan, X.; Wei, Q.; Lieber, C. M. *Science* **2001**, *291*, 630–633.
- (23) Huang, J.; Fan, R.; Connor, S.; Yang, P. *Angew. Chem., Int. Ed.* **2007**, *46*, 2414–2417.

happens if we mix nanoparticles of different sizes together, or nanorods with different aspect ratios, or mix nanowires with nanoplatelets? Shevchenko and co-workers mixed two sets of spherical nanoparticles with different sizes and compositions and observed the formation of binary superlattices isostructural with atomic crystal structures such as NaCl.<sup>25,26</sup> Ming and co-workers studied the assembly of binary mixtures of Au nanorods with different aspect ratios and observed that the nature of the superstructure is controlled by the nanorod diameters.<sup>27</sup> With the same average diameter, the two nanorod samples mixed to form nematic superstructures without self-separation. With different average diameters, self-separation occurred. van der Kooij and Lekkerkerker studied the rod–plate mixed colloids and observed an exceptionally rich phase diagram including the coexistence of up to four liquid crystal phases.<sup>28</sup> Despite the above interesting results, the coassemblies of multicomponent colloids have remained relatively unexplored experimentally.

In this contribution, we study the coassembly of nanowires and graphene oxide nanosheets. Graphene oxide (GO) is an ultrathin two-dimensional structure consisting of intact aromatic domains interspersed with hydroxyl and epoxy functional groups on the top and bottom sides of each sheet, surrounded by carboxyl groups in the periphery.<sup>29</sup> The GO nanosheets, synthesized by oxidizing and exfoliating graphite crystals,<sup>30,31</sup> can be easily dispersed in water and processed into papers,<sup>32</sup> films, and composites.<sup>33,34</sup> Moreover, GO can be reduced into graphene, which is attractive for applications in electronics,<sup>35,36</sup> sensing,<sup>37,38</sup> and transparent conducting electrodes.<sup>34,39,40</sup>

An interesting phenomenon observed in our study is the formation of large-area, unidirectional self-alignment of nanowires at the air–water interface with the addition of GO nanosheets to the nanowire dispersion. The aligned nanowires can be transferred to hydrophilic substrates with their orientation parallel to the liquid–substrate contact line upon the evaporation

of water. We believe that the interactions between GO and nanowires, mainly hydrogen bonding and ion–dipole interactions, modify the surface properties of nanowires and lead to their enrichment at the solution surface. When a critical surface concentration is reached, the nanowire self-alignment occurs.

## Materials and Methods

**Preparation of Na<sub>0.44</sub>MnO<sub>2</sub> Nanowires.** Na<sub>0.44</sub>MnO<sub>2</sub> nanowires were synthesized by the hydrothermal method as reported elsewhere.<sup>41</sup> Briefly, 0.5 mmol of Mn<sub>2</sub>O<sub>3</sub> powder was mixed with 10 mL of 5 M NaOH solution and magnetically stirred for 10 min. The suspension was transferred to a 23 mL Teflon-lined autoclave and reacted at 210 °C for 4 days. Nanowire products were washed thoroughly with water first and then ethanol to remove residual NaOH until the final solution pH was <11. They were dried in air.

**Preparation of GO Sheets.** GO sheets were synthesized by a modified Hummers' method.<sup>31</sup> It started with graphite pretreatment. To accomplish this, 12 g of graphite powder were added to an 80 °C solution of 50 mL of concentrated H<sub>2</sub>SO<sub>4</sub>, 10 g of K<sub>2</sub>S<sub>2</sub>O<sub>8</sub>, and 10 g of P<sub>2</sub>O<sub>5</sub>. The mixture was reacted for 6 h, after which it was diluted with 2 L of water, filtered, and washed using a 0.2 μm Nylon Millipore filter and dried in air overnight. For the following oxidation step, 460 mL of H<sub>2</sub>SO<sub>4</sub> were chilled to 0 °C using an ice bath. The oxidized graphite was added to the acid and stirred. Then, 60 g of KMnO<sub>4</sub> were added slowly with temperature controlled below 10 °C. This mixture was allowed to react at 35 °C for 2 h, after which 920 mL of distilled water were added slowly so as to keep the temperature below 50 °C. After further reaction for 2 h, 2.8 L of water and 50 mL of 30% H<sub>2</sub>O<sub>2</sub> were added, resulting in a brilliant yellow color along with bubbling. The mixture was allowed to settle for at least a day before the supernatant was decanted. The remaining mixture was then centrifuged and washed with a total of 5 L of 10% HCl solution followed by 5 L of water to remove the acid. The resulting solid was subjected to dialysis for a week to remove remaining metal ions and acids. Finally, the product was vacuum-dried.

**Nanowire Self-Alignment.** In a typical experiment, 5 mg of GO were first dispersed in 10 mL of water contained in a glass vial of 1 in. diameter with magnetic stirring and sonication. Then 25 mg of Na<sub>0.44</sub>MnO<sub>2</sub> nanowires were added and continuously stirred for 2 h. Solution pH was carefully adjusted to 9.0–9.5 with diluted HCl or ammonia. Afterwards, the solution was subjected to cup-horn sonication for a total time of 5 min to achieve a homogeneous nanowire/GO dispersion. This was indicated by a uniform brown color of the solution and evident birefringence when shaken or sonicated. Piranha-cleaned Si wafer slices were used as the substrates and immersed in solution standing vertically against the vial wall. The whole vial was then placed in an oven with a heating temperature set at 60 °C and left overnight for evaporation.

**Characterizations.** Scanning electron microscope (SEM) images and energy dispersive X-ray (EDX) elemental mapping of nanowire self-alignment patterns were recorded on Sirion SEM. We carried out the droplet test by loading one droplet of solution on a transparent glass slide, closely monitoring its drying process under a Nikon Eclipse LV100 optical microscope connected to a digital camera (Digital Sight DS-2Mv). Zeta-potentials were measured on a Zetasizer Nano ZS90. Sessile drop contact angle measurements were done under ambient temperature on a Krüss Easy Drop Standard System DSA100 by adding water to the sample surface with a motor-driven syringe. Raman spectra were measured on a Renishaw Smith Raman IR microprobe spectrometer with an excitation wavelength of 514 nm.

## Results and Discussion

**Nanowire Colloidal Stability.** We selected Na<sub>0.44</sub>MnO<sub>2</sub> nanowires for our study due to their ease of synthesis, high reaction

- (24) van der Kooij, F. M.; Kassapidou, K.; Lekkerkerker, H. N. W. *Nature (London)* **2000**, *406*, 868–871.
- (25) Shevchenko, E. V.; Talapin, D. V.; Kotov, N. A.; O'Brien, S.; Murray, C. B. *Nature (London)* **2006**, *439*, 55–59.
- (26) Shevchenko, E. V.; Talapin, D. V.; Murray, C. B.; O'Brien, S. *J. Am. Chem. Soc.* **2006**, *128*, 3620–3637.
- (27) Ming, T.; Kou, X.; Chen, H.; Wang, T.; Tam, H.-L.; Cheah, K.-W.; Chen, J.-Y.; Wang, J. *Angew. Chem., Int. Ed.* **2008**, *47*, 9685–9690.
- (28) van der Kooij, F. M.; Lekkerkerker, H. N. W. *Phys. Rev. Lett.* **2000**, *84*, 781–784.
- (29) Szabo, T.; Berkesi, O.; Forgo, P.; Josepovits, K.; Sanakis, Y.; Petridis, D.; Dekany, I. *Chem. Mater.* **2006**, *18*, 2740–2749.
- (30) Hummers, W. S., Jr.; Offeman, R. E. *J. Am. Chem. Soc.* **1958**, *80*, 1339.
- (31) Kovtyukhova, N. I.; Ollivier, P. J.; Martin, B. R.; Mallouk, T. E.; Chizhik, S. A.; Buzaneva, E. V.; Gorchinskiy, A. D. *Chem. Mater.* **1999**, *11*, 771–778.
- (32) Dikin, D. A.; Stankovich, S.; Zimney, E. J.; Piner, R. D.; Dommett, G. H. B.; Evmenenko, G.; Nguyen, S. T.; Ruoff, R. S. *Nature (London)* **2007**, *448*, 457–460.
- (33) Stankovich, S.; Dikin, D. A.; Dommett, G. H. B.; Kohlhaas, K. M.; Zimney, E. J.; Stach, E. A.; Piner, R. D.; Nguyen, S. T.; Ruoff, R. S. *Nature (London)* **2006**, *442*, 282–286.
- (34) Watcharotone, S.; Dikin, D. A.; Stankovich, S.; Piner, R.; Jung, I.; Dommett, G. H. B.; Evmenenko, G.; Wu, S.-E.; Chen, S.-F.; Liu, C.-P.; Nguyen, S. T.; Ruoff, R. S. *Nano Lett.* **2007**, *7*, 1888–1892.
- (35) Geim, A. K.; Novoselov, K. S. *Nat. Mater.* **2007**, *6*, 183–191.
- (36) Li, X. L.; Wang, X. R.; Zhang, L.; Lee, S. W.; Dai, H. J. *Science* **2008**, *319*, 1229–1232.
- (37) Robinson, J. T.; Perkins, F. K.; Snow, E. S.; Wei, Z.; Sheehan, P. E. *Nano Lett.* **2008**, *8*, 3137–3140.
- (38) Schedin, F.; Geim, A. K.; Morozov, S. V.; Hill, E. W.; Blake, P.; Katsnelson, M. I.; Novoselov, K. S. *Nat. Mater.* **2007**, *6*, 652–655.
- (39) Becerril, H. A.; Mao, J.; Liu, Z.; Stoltenberg, R. M.; Bao, Z.; Chen, Y. *ACS Nano* **2008**, *2*, 463–470.
- (40) Wang, X.; Zhi, L.; Muellen, K. *Nano Lett.* **2008**, *8*, 323–327.

- (41) Li, Y.; Wu, Y. *Nano Res.* **2009**, *2*, 57–66.

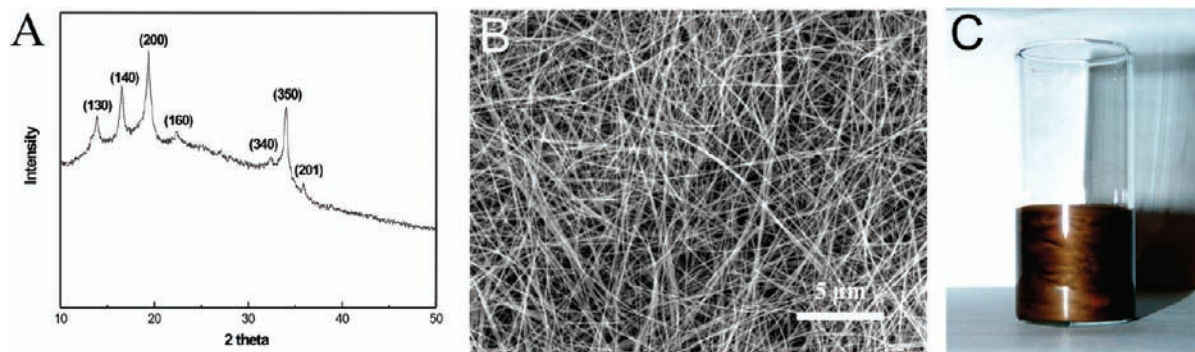


**Figure 1.** As-prepared  $\text{Na}_{0.44}\text{MnO}_2$  nanowires. (A) XRD pattern of the as-prepared nanowire powders corresponding to the standard  $\text{Na}_{0.44}\text{MnO}_2$  (PDF # 27-0750). (B) SEM image showing nanowire high aspect ratio and (C) photo of nanowire solution being magnetically stirred.

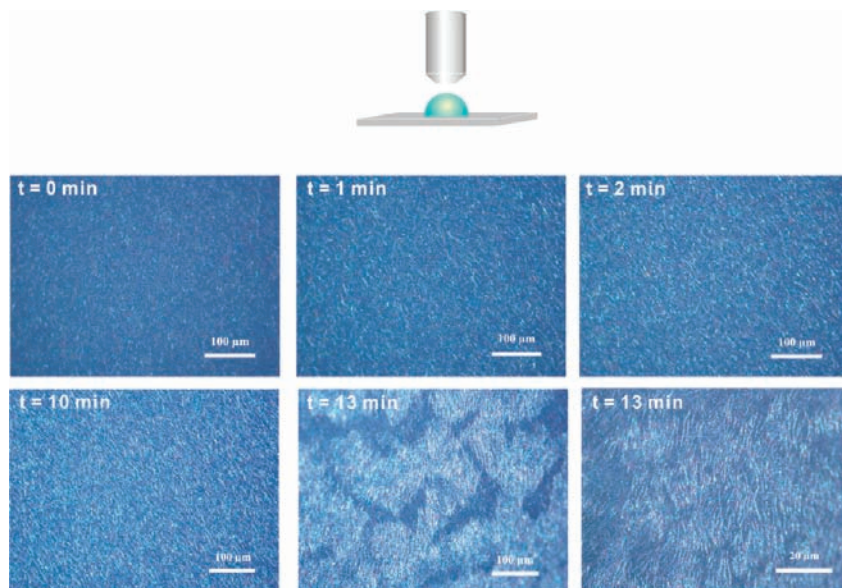


**Figure 2.** Nanowire self-alignment at the solution surface. In the droplet test, a droplet of GO-nanowire mixed suspension was loaded onto a piece of glass slide and observed through an optical microscope (top schematic diagram). Accompanying its slow drying process, nanowires are gradually transported to surface and self-aligned (bottom 6 pictures, nanowires shown as white shiny lines). GO concentration is 0.5 mg/mL in this test.

yield, and large aspect ratio (Figure 1).<sup>41</sup> Most are more than 10  $\mu\text{m}$  in length and  $\sim 50$  nm in width. These nanowires are easily dispersed in aqueous medium assisted by sonication and form stable colloidal solutions (Figure 1C).

Nanowire colloidal stability is important to ensure the high-quality alignment. It is sensitive to the solution pH. At pH = 9.0–9.5, the nanowire solution is stable for months with negligible sedimentation observed. This great stability stems from the mutual coulombic repulsion between negatively charged nanowire surfaces as confirmed by the measured negative zeta-potential. However, the colloid is destabilized by acidifying the solution with diluted HCl below a critical pH of 8.0–9.0, and nanowire aggregation occurs. Destabilized nanowire aggregates can be reversibly redispersed by tuning the solution pH back up with diluted ammonia along with mild sonication. No difference in the solution was identified when the pH was raised above 9.5. However, Si wafer or glass substrates start to be etched beyond this point. Based on the above considerations, the solution pH was strictly controlled in the narrow window 9.0–9.5 for this study.

**Nanowire Enrichment and Alignment at Air–Liquid Interface.** We first prepared a mixed colloidal solution containing both GO and nanowires. The typical concentration is that 1 mL of solution contains 2.5 mg of nanowires and 0.5 mg of GO

nanosheets. We then dropped a droplet of the mixed suspension onto a piece of glass slide and followed its drying process using an optical microscope at room temperature (Figure 2). We focused on the top surface of the droplet, where nanowires appeared as shiny white wires when viewed in the reflection mode due to their light scattering. During evaporation, the surface concentration of nanowires gradually increased with time, and later they formed nematic ordering with the wires pointing in one direction. Eventually, these individual nanowires grew to “islands” and further merged to form a compact film across the entire solution surface (Figure 2, see also Supporting Information, Figure S1, images taken in the transmission mode). This droplet experiment clearly shows that nanowires are enriched at the surface as the solution evaporates. After a certain surface accumulation is reached, orientational ordering occurs, resulting in a continuous film of self-aligned nanowires.

**Nanowire Alignment on Substrates.** The aligned nanowires can be transferred to a substrate by solvent evaporation. For this purpose, the GO–nanowire mixed suspension was contained in a vial with a piece of Si wafer standing vertically inside. The solution was heated at 60  $^{\circ}\text{C}$ . After the water completely evaporated, we observed unidirectional nanowire alignment over

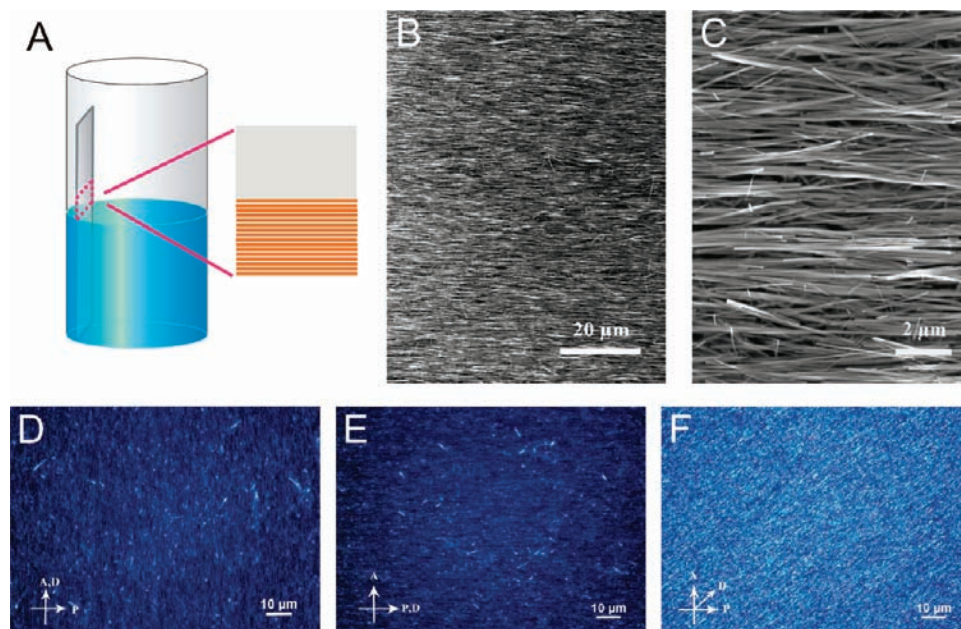


**Figure 3.** Nanowire alignment with GO on a Si substrate. (A) The scheme showing experimental setup: a piece of cleaned Si wafer is immersed into the well-dispersed nanowire/GO solution. Upon solution evaporation, aligned nanowire pattern is deposited on the substrate with the orientation parallel to the horizontal liquid–substrate contact line. (B and C) typical SEM images of nanowire alignment pattern. (D–F) Cross-polarized optical microscope pictures of self-aligned nanowires with the nanowire director (D) parallel to, (E) vertical to, and (F) 45° to the polarizer. A, P, and D represent analyzer, polarizer, and nanowire director (orientation) respectively.

the entire Si wafer substrate with nanowires oriented horizontally, i.e., parallel to the liquid–substrate contact line (Figure 3).

The quality of alignment was also evaluated qualitatively with cross-polarized optical microscopy. Figure 3D–F presents typical pictures of a self-aligned nanowire film observed for various angles between the nanowire alignment director and the polarizer direction. As expected for a homogeneous alignment of one-dimensional materials, dark pictures were observed when the nanowire director was parallel or vertical to the polarizer, while the brightest picture was observed when it was 45° to the polarizer.

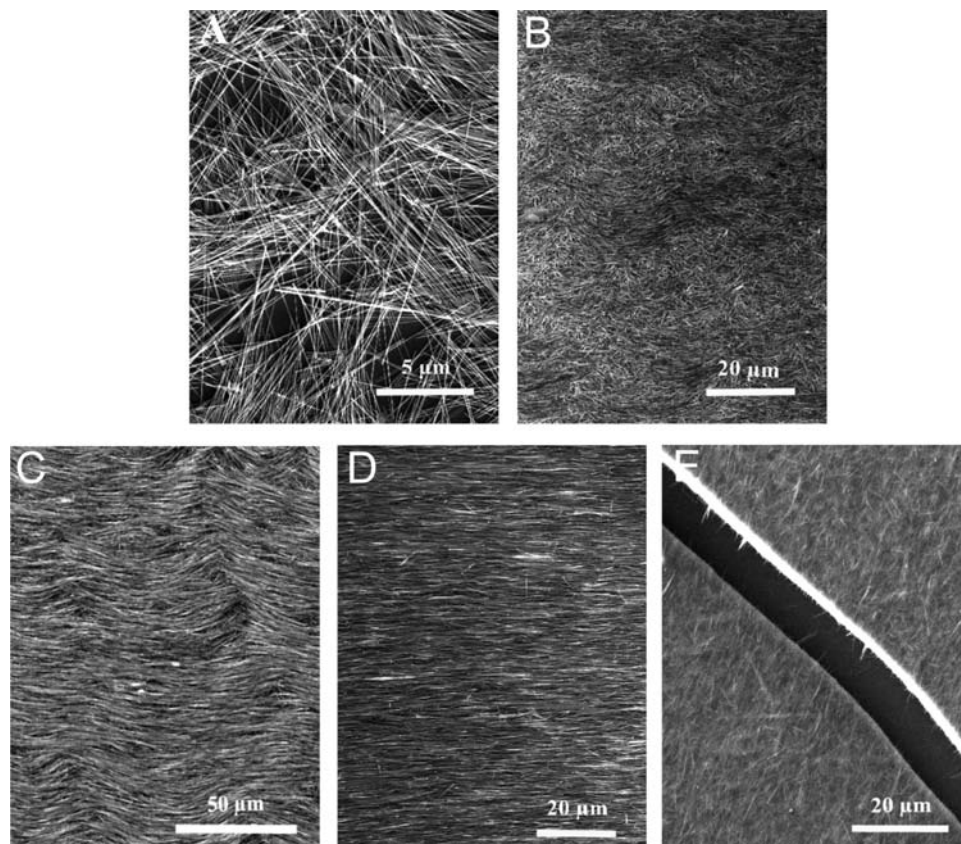
**Crucial Role of GO for Nanowire Alignment.** We have done control experiments to confirm that GO plays a crucial role in the nanowire alignment. In its absence or with its amount <0.13 mg/mL, random nanowire deposition was observed (Figure 4A). No nanowire surface enrichment was observed in the droplet evaporation experiment either (Supporting Information, Figure S2). The quality of nanowire alignment improves with the increasing amount of GO up to 1.3 mg/mL (Figure 4B–D), while adding too much (e.g., 2.5 mg/ml) gives rise to gelatinous composite films (Figure 4E). We have also done compositional mapping by using EDX and Raman spectroscopy to prove that GO nanosheets have been codeposited on the substrate with the nanowires (Figure 5). The typical EDX spectrum (Figure 5A) shows a strong carbon peak, and the distribution of carbon is consistent with the contour of nanowires (comparing Figure 5B and 5C). The Raman spectrum also shows the coexistence of GO and nanowires in the aligned nanowire film (Figure 5D).

**Interaction Between GO and Nanowires.** The essential role of GO in nanowire alignment indicates a strong interaction between GO nanosheets and  $\text{Na}_{0.44}\text{MnO}_2$  nanowires that modifies the behavior of nanowires. It is well-known that polymeric

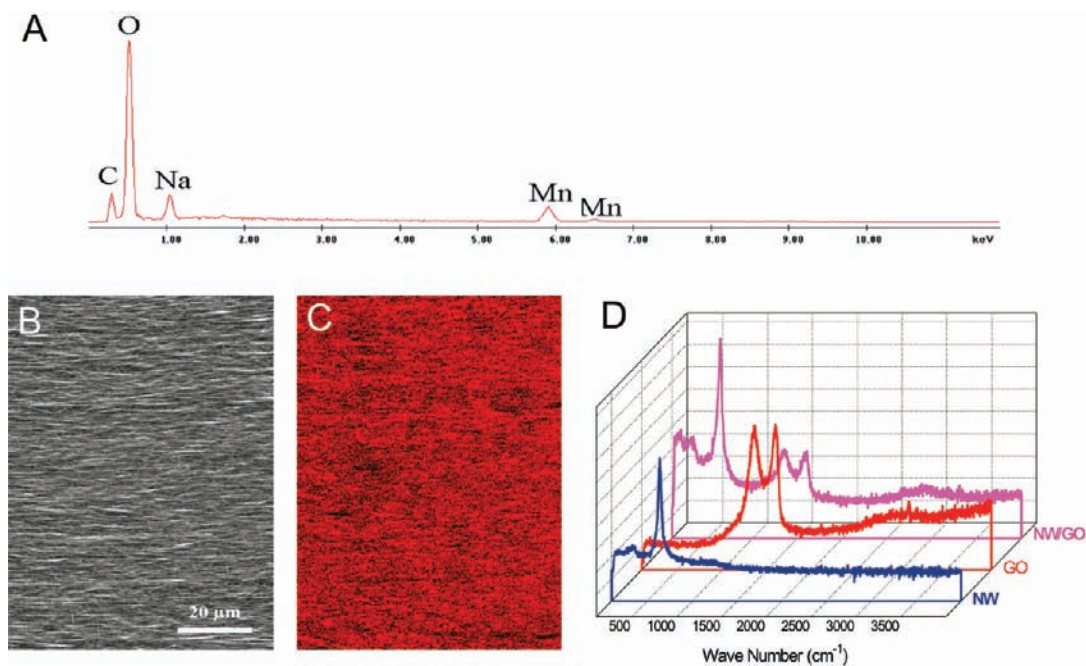
macromolecules can adsorb on the surface of oxides.<sup>42</sup> For example, poly(acrylic acid) and polyacrylamide have been reported to adsorb on  $\text{MnO}_2$  (which has a very similar surface nature to  $\text{Na}_{0.44}\text{MnO}_2$ ) through hydrogen-bond interactions in a wide pH range in aqueous solution.<sup>43</sup> GO nanosheets can be treated as two-dimensional macromolecules. The basal plane is electrically neutral with rich hydroxyl and epoxy groups.<sup>29</sup> Therefore, it is reasonable to suggest that the basal plane of a GO nanosheet can adsorb on nanowires through hydrogen bonding and ion–dipole interactions. For example, the epoxy groups on GO can bond preferentially to Mn–OH surface sites exposed on nanowire surfaces, and the hydroxyl groups on GO can form attractive ion–dipole interactions with Mn–O<sup>−</sup> active sites (Scheme 1A). Moreover, each GO sheet is ultrathin and flexible. It can easily deform itself to facilitate the multisite contacts with the same nanowire to increase the affinity of GO for the nanowire (Scheme 1B). Although GO nanosheets carry negative charges, the charges are located only at the edges of the nanosheets due to the ionization of carbonyl groups.<sup>29</sup> Therefore, the electrostatic repulsion between the nanosheet edges and the nanowire surface can be minimized by orienting the edges away from the nanowire surface. We have measured the zeta-potential of the nanowire solution and found it became more negative from −54 to −58 mV after the addition of GO (Supporting Information, Figure S3). The increase in the surface negative charge is consistent with our model of GO adsorption onto nanowires.<sup>43</sup> We have also observed the presence of GO nanosheets around nanowires in TEM characterizations (Supporting Information, Figure S4).

**Mechanism of Nanowire Surface Enrichment and Alignment.** The GO adsorption on nanowires discussed in the last section can result in the modification of the surface properties of nanowires. Bare nanowires are superhydrophilic. They have

(42) Napper, D. H. *Polymeric Stabilization of Colloidal Dispersions*; Academic Press: London, 1983.



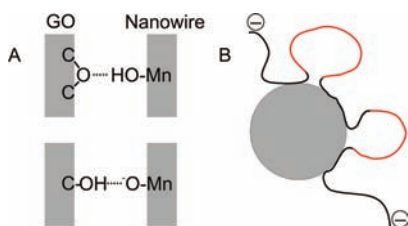
**Figure 4.** Effect of different GO concentrations on the quality of nanowire alignment: (A) 0, (B) 0.13, (C) 0.25, (D) 1.3, and (E) 2.5 mg/mL. Ordered self-alignment pattern could be achieved by adding 0.25–1.3 mg/mL GO. Lower concentrations yield random nanowire patterns, while increasing its concentration beyond this range gives rise to the gelatinous composite film.



**Figure 5.** EDX and Raman characterization as evidence of GO–nanowire codeposition in aligned nanowire film. (A–C) Elemental mapping of the carbon distribution in the aligned nanowires prepared with 1.3 mg/mL GO solution. (A) A typical EDX spectrum, (B) an SEM image, and (C) the corresponding carbon mapping image using carbon-k line. No apparent carbon peak could be detected in the EDX when GO concentration is below 0.13 mg/mL. (D) Raman spectra of (blue) pure nanowires (NW), (red) pure GO, and (magenta) the aligned nanowire/GO composite (NW/GO). The aligned nanowire film shows characteristic peaks of both nanowires and GO nanosheets.

no measurable water contact angle: once a water droplet is loaded onto a nanowire film, it spreads out entirely. On the

contrary, the GO film is less hydrophilic due to the prevailing C–C or C=C bonds in the sheet. Its water contact angle was

**Scheme 1.** Interactions between GO and Nanowires<sup>a</sup>

<sup>a</sup> (A) Examples of hydrogen bonding and ion-dipole interactions between GO and nanowire. (B) Schematic conformation of a GO nanosheet adsorbed on a nanowire surface. For clarity, the GO is represented by a linear polymer, and the nanowire represented by its circular cross section. The red color on GO indicates intact aromatic regions.

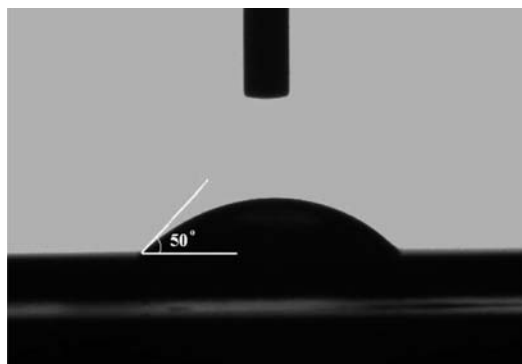


**Figure 6.** Water contact angle measurement of the GO film gives a value of 50°. This is in contrast to the superhydrophilic nanowire film which shows no measurable contact angle.

measured to be 50° (Figure 6). One recent study confirmed that GO was surface-active and its Langmuir–Blodgett film was prepared.<sup>44</sup> Consequently, it is reasonable to expect that the adsorption of GO on nanowires will render the latter surface “active” and thus induce their surface enrichment.

We built a quantitative model to analyze nanowire surface energy in solution in an effort to spot the origin of the observed nanowire surface enrichment (Supporting Information, Modeling and Calculations).<sup>45</sup> Under the long nanowire approximation ( $l \gg d$ ), calculations show that the surface energy change ( $\Delta\mu$ ) for a nanowire going from bulk solution to the solution–air interface equals  $\Delta\mu = dl\gamma(\theta_c \cos \theta_c - \sin \theta_c)$ , where  $d$  and  $l$  are the nanowire diameter and length, respectively,  $\gamma$  is the water surface tension, and  $\theta_c$  is the water contact angle of nanowires. For bare nanowires,  $\Delta\mu$  is zero since  $\theta_c \approx 0^\circ$ . In the case of GO-adsorbed nanowires,  $\Delta\mu$  is on the order of  $-10^{-14}$  J, assuming  $d = 100$  nm,  $l = 10$   $\mu\text{m}$ , and  $\theta_c = 50^\circ$ . The decrease of surface energy will, therefore, drive GO-adsorbed nanowires to the solution surface.<sup>45</sup>

On the other hand, the random Brownian motion of nanowires can move the surface nanowires back into the bulk solution. This will interplay with the trapping of nanowires at the surface and thus lead to an average surface residence time ( $\tau$ ). If we treat the surface nanowires as in a harmonic potential well with a depth of  $|\Delta\mu|$ , their average residence time would have an exponential dependence on the potential depth,  $\tau \approx \exp(|\Delta\mu|/k_B T)$ , where  $k_B$  is the Boltzmann constant and  $T$  is the

temperature.<sup>46</sup> At room temperature,  $k_B T$  ( $\sim 10^{-21}$  J) is much smaller than our calculated  $|\Delta\mu|$ ; therefore, once the GO-adsorbed nanowires move to the solution surface, they will be confined there, which explains the observed nanowire surface enrichment. The transfer of nanowires to the solution surface should be facilitated by the upward convective flow in the solution, developed to replenish the surface liquid lost due to evaporation.<sup>47</sup>

Surface enrichment paves the way for the subsequent nanowire self-alignment observed in our droplet test after a certain critical surface concentration is reached. According to the two-dimensional Onsager’s model, the isotropic-to-nematic phase transition occurs at a nanowire surface concentration of  $C_o = \alpha/l^2$ , where  $\alpha$  is a constant calculated to be 4.7 and  $l$  is the length of the nanowire.<sup>48</sup> The critical nanowire surface density  $C_o$  is thereby on the order of  $10^6$   $\text{cm}^{-2}$  considering a nanowire length of 10  $\mu\text{m}$ . This only requires a small fraction ( $\sim 0.1\%$ ) of total nanowires to be raised to the solution surface and trapped there. The Onsager model assumes that the only important force between nanowires is the steric force. If we take into account the electrostatic repulsion between our nanowires, the critical surface concentration  $C_o$  will be even lower.

Through the above analysis, we can identify several key structural features of GO nanosheets for nanowire alignment. First, GO sheets have interspersed hydrophilic and hydrophobic regions: the rich hydrophilic functional groups facilitate the attachment of GO onto nanowires through hydrogen bonding, while hydrophobic regions render the GO-adsorbed nanowires surface-active properties. The flexibility of the 2D macromolecules also facilitates multisite contact to increase the GO affinity for nanowires. Second, GO nanosheets carry negative charges at our experimental conditions. Therefore, GO attachment increases the colloidal stability of nanowires as confirmed by the zeta-potential measurement. This will prevent the quick and random agglomeration of nanowires and thus allow the time and freedom for nanowire alignment. To demonstrate the uniqueness of GO in our experiment, different surfactants were tested as alternatives under identical experimental conditions. This includes cationic hexadecyltrimethylammonium bromide (CTAB), anionic sodium dodecylbenzenesulfate (SDS), sodium dioctylsulfosuccinate (AOT), and nonionic polyvinylpyrrolidone (PVP,  $M_w = 10,000$ ). Although we have observed the surface enrichment of nanowires during the droplet tests using these nanowires, the nanowires tend to aggregate, showing no sign of alignment (Supporting Information, Figures S5 and S6). This can be explained by the attractive hydrophobic interactions between the surfactant tails. These control experiments show that the dual roles of GO as both the surface “activator” and the colloidal “stabilizer” are essential for nanowire alignment.

Finally we would like to point out the basic difference between our nanowire alignment and the “coffee stain” effect<sup>47</sup> reported earlier for nanowire alignment. In the “coffee stain” effect, nanowires were carried by capillary flows and, therefore, were observed to orient perpendicularly to the liquid–substrate contact line.<sup>23</sup> In our experiment, the nanowires are aligned due

(43) Chibowski, S.; Wisniewska, M.; Paszkiewicz, M. *Adsorpt. Sci. Technol.* **2002**, *20*, 511–522.

(44) Cote, L. J.; Kim, F.; Huang, J. *J. Am. Chem. Soc.* **2009**, *131*, 1043.

(45) Sun, B.; Siringhaus, H. *J. Am. Chem. Soc.* **2006**, *128*, 16231–16237.

(46) Bigioni, T. P.; Lin, X.-M.; Nguyen, T. T.; Corwin, E. I.; Witten, T. A.; Jaeger, H. M. *Nat. Mater.* **2006**, *5*, 265–270.

(47) Deegan, R. D.; Bakajin, O.; Dupont, T. F.; Huber, G.; Nagel, S. R.; Witten, T. A. *Nature (London)* **1997**, *389*, 827–829.

(48) Frenkel, D.; Eppenga, R. *Phys. Rev. A* **1985**, *31*, 1776–87.

to the surface enrichment and are parallel to the liquid–substrate contact line due to its templating effect.

### Conclusion

In this work, we have studied the coassembly behavior of GO nanosheets and nanowires. We observed the concentration enrichment and alignment of nanowires at the air–water interface with the addition of GO nanosheets to the nanowire dispersion. The aligned nanowires can be transferred to hydrophilic substrates with their orientation parallel to the liquid–substrate contact line upon evaporation of the solvent. GO nanosheets can be thought of as soft 2D macromolecules. Through hydrogen bonding and ion–dipole interactions, GO nanosheets can adsorb onto the nanowire surface and thereby change the surface properties. As a result, the GO-adsorbed nanowires can be surface active and become enriched at the air–water interface. When a critical concentration is reached, the alignment of nanowires occurs according to Onsager's theory. This study brings about a new application of GO in colloidal chemistry and a novel method to achieve large-area,

unidirectional alignment of nanowires. This method has been extended to align other oxide nanowires such as sodium titanate and TiO<sub>2</sub> nanowires (Supporting Information, Figure S7).

**Acknowledgment.** We would like to thank Elvin Beach and Dr. Patricia A. Morris for help in contact angle measurements as well as Mingming Ma and Dr. Dennis Bong for help in zeta-potential measurements. Y.W. acknowledges support from the U.S. Department of Energy under the Award No. DE-FG02-07ER46427 and Research Corporation Cottrell Scholar Award.

**Supporting Information Available:** Modeling and calculations, aligned nanowires in the droplet test viewed in the transmission mode, the droplet test results without GO addition, zeta-potential measurements, evidence of GO around nanowires in TEM, the droplet test results with the addition of common surfactants, sodium titanate nanowire alignment, and complete ref 15. This material is available free of charge via the Internet at <http://pubs.acs.org>.

JA9000882